CT-Invariant Quantum Spin Hall Effect in Ferromagnetic Graphene

Qing-feng Sun[1,*] and X. C. Xie[1,2]

[1]*Institute of Physics, Chinese Academy of Sciences, Beijing 100190, China*
[2]*Department of Physics, Oklahoma State University, Stillwater, Oklahoma 74078, USA*
(Received 13 July 2009; published 12 February 2010)

We predict a quantum spin Hall effect (QSHE) in ferromagnetic graphene under a magnetic field. Unlike the previous QSHE, this QSHE appears in the absence of spin-orbit interaction and thus, is arrived at from a different physical origin. The previous QSHE is protected by the time-reversal (T) invariance. This new QSHE is protected by CT invariance, where C is the charge conjugation operation. Because of this QSHE, the longitudinal resistance exhibits quantum plateaus. The plateau values are at $1/2$, $1/6$, $3/28$, ..., (in units of h/e^2), depending on the filling factors of the spin-up and spin-down carriers. The spin Hall resistance is also investigated and is found to be robust against the disorder.

In the years since the spin Hall effect (SHE) has been discovered, it has generated great interest [1–4]. In the SHE, an applied longitudinal charge current or voltage bias induces a transverse spin current due to the spin-dependent scatterings [1,2] of the spin-orbit interaction (SOI) [3]. Soon afterwards, the quantum SHE (QSHE) was also predicted [5,6]. The QSHE occurs in a topological insulator in which the bulk material is an insulator with two helical edge states carrying the current [7]. The edge states, with opposite spins on a given edge or opposite edges for a given spin direction containing opposite propagation directions, lead to a quantized spin Hall conductance. The QSHE is a new quantum state of matter with a nontrivial topological property. The existence of QSHE was first proposed in a graphene film in which the SOI opened a band gap and established the edge states [5,6]. But the subsequent work found that the SOI in the graphene was quite weak and the gap opening was small, so the QSHE was difficult to observe [8]. Soon afterwards, the QSHE was also predicted to exist in some other systems [9–12]. Recently, the QSHE was successfully realized in the CdTe/HgTe/CdTe quantum wells, and a quantized longitudinal resistance plateau was experimentally observed due to the QSHE [11].

Another subject that has also been extensively investigated in recent years is graphene, a single-layer hexagonal lattice of carbon atoms [13], after it has been successfully fabricated [14,15]. Graphene has a unique band structure with a linear dispersion near the Fermi surface, giving it many peculiar properties. For example, the quasiparticles obey the Dirac-like equation and have relativisticlike behaviors, and its Hall plateaus are at the half-integer values.

In this Letter, we predict a new kind of QSHE in a ferromagnetic graphene. Let us first imagine a two-dimensional system consisting of the following characteristics: (i) its carriers contain electrons and holes; (ii) both electrons and holes are completely spin-polarized with opposite spin polarizations. When a high perpendicular magnetic field is applied to the system, the edge states

are formed and the carriers move only along the edges. In particular, the electrons (with their spins up) and holes (with their spins down) move in opposite directions on a given edge [see the inset in Fig. 1(a)]. Therefore, the QSHE automatically exists in this system. Although the ordinary metals (or doped semiconductors) cannot meet the above two characteristics, a ferromagnetic graphene does. Recently, several approaches to realize a ferromagnetic graphene have been suggested [16–18]. For example, the ferromagnetic graphene can be realized by growing the graphene on a ferromagnetic insulator (e.g., EuO) [17]. For a ferromagnetic graphene, as soon as the Fermi energy E_F is tuned to lie between the spin-up and spin-down Dirac
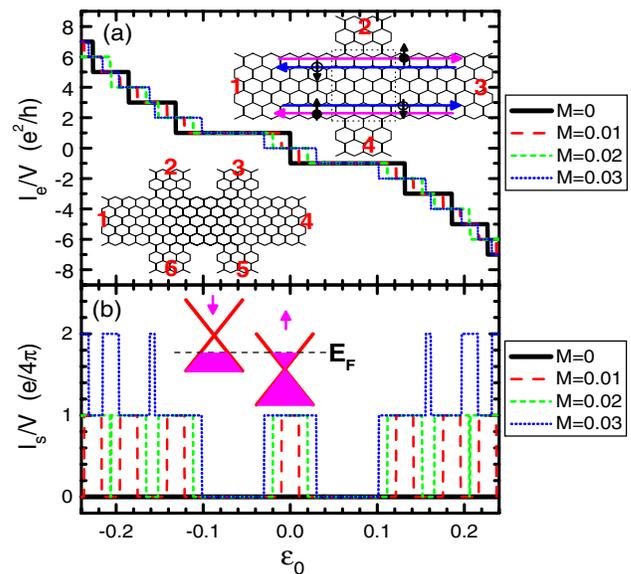
FIG. 1 (color online).   The Hall conductance I_e/V (a) and spin Hall conductance I_s/V (b) vs. the energy ϵ_0 for $N = 80$ and $\phi = 0.005$. The two insets in (a) are the schematic diagram for the four- and six-terminal graphene's Hall bars. The inset in (b) is the schematic diagram for band structure of the ferromagnetic graphene while $\epsilon_0 + M > E_F > \epsilon_0 - M$.

points [see the inset in Fig. 1(b)], the above two characteristics are met and the QSHE occurs. In the following calculations, we consider four- and six-terminal graphene Hall bars (see the insets in Fig. 1(a)]. The results reveal that the transverse spin current and spin Hall resistance indeed show the quantized plateaus because of the QSHE.

Comparing this new QSHE with the previously-studied QSHE, there are two essential differences: (i) The previous QSHE comes from the SOI and the proposed systems all contain the time-reversal symmetry [5–7,9,10], while the present QSHE exists without the SOI and breaks the time-reversal symmetry. However, this new QSHE is protected by CT invariance. (ii) In the previous QSHE, the edge states only carry a spin current while at equilibrium; in this QSHE system, the edge states carry both spin and charge currents at equilibrium with the two edges states being CT partners of each other [see the inset in Fig. 1(a)]. Thus, this is a new kind of QSHE and the system is a new type of topological insulator. Because of the topological invariance, the plateaus of the spin Hall resistance are robust to disorder or impurity scattering. So the plateau is very stable and its value can be used as the standard value for the spin Hall resistance.

In the tight-binding representation, the four- or six-terminal ferromagnetic graphene device [see the insets in Fig. 1(a)] can be described by the Hamiltonian [19]

$$H = \sum_{i,\sigma}(\epsilon_0 - \sigma M)a_{i\sigma}^\dagger a_{i\sigma} - \sum_{\langle ij\rangle,\sigma} te^{i\phi_{ij}}a_{i\sigma}^\dagger a_{j\sigma}, \quad (1)$$

where $a_{i\sigma}$ and $a_{i\sigma}^\dagger$ are the annihilation and creation operators at the discrete site i. ϵ_0 is the on-site energy (i.e., the Dirac-point energy), M is the ferromagnetic exchange split [17], and t is the nearest neighbor hopping element. Here, the whole device, including the center region and four or six terminals, is made of the ferromagnetic graphene. With the presence of a perpendicular magnetic field B, a phase factor ϕ_{ij} is added to the hopping element, $\phi_{ij} = \int_i^j \vec{A} \cdot d\vec{l}/\phi_0$ with the vector potential $\vec{A} = (-By, 0, 0)$ and $\phi_0 = \hbar/e$.

The transmission coefficient $T_{pq\sigma}(\epsilon)$ from the terminal q to the terminal p with spin σ can be calculated from the equation [20] $T_{pq\sigma}(\epsilon) = \text{Tr}[\Gamma_{p\sigma}G_\sigma^r\Gamma_{q\sigma}G_\sigma^a]$, where $\Gamma_{p\sigma}(\epsilon) = i[\Sigma_{p\sigma}^r(\epsilon) - \Sigma_{p\sigma}^a(\epsilon)]$, the Green functions $G_\sigma^r(\epsilon) = [G_\sigma^a(\epsilon)]^\dagger = 1/[\epsilon - H_\sigma^{cen} - \sum_p\Sigma_{p\sigma}^r]$, and H_σ^{cen} is the Hamiltonian of the center region. The retarded self-energy $\Sigma_{p\sigma}^r(\epsilon)$ due to the coupling to the terminal p can be calculated numerically [21]. After obtaining the transmission coefficient, the particle current in the terminal p with the spin σ can be calculated from the Landauer-Büttiker formula $I_{p\sigma} = (1/h) \int d\epsilon \sum_q T_{pq\sigma}(\epsilon) \times [f_{q\sigma}(\epsilon) - f_{p\sigma}(\epsilon)]$, where $f_{p\sigma}(\epsilon) = 1/\{\exp[(\epsilon - \mu_{p\sigma})/k_BT] + 1\}$ is the Fermi distribution function in the terminal p, with the spin-dependent chemical potential $\mu_{p\sigma}$ and the temperature T. In the following numerical calculations, we take $t = 1$ as the energy unit and only

consider the zero temperature case ($T = 0$), as the thermal energy k_BT is normally much smaller than other energy scales in the problem. The sample width is denoted by N, and the insets of Fig. 1(a) show a system with $N = 3$. In the calculations, we choose $N = 80$ and 40, and the corresponding widths are 33.9 and 16.9 nm. The magnetic field is described by the ϕ with $\phi \equiv (3\sqrt{3}/4)a^2B/\phi_0$ and the magnetic flux in a honeycomb lattice is 2ϕ.

We first consider the four-terminal device (see the inset at the top right corner of Fig. 1(a) and a small bias V is applied between the longitudinal terminals 1 and 3 to study the induced charge current I_{ne} [$I_{ne} \equiv e(I_{n\uparrow} + I_{n\downarrow})$] and spin current I_{ns} [$I_{ns} \equiv (\hbar/2)(I_{n\uparrow} - I_{n\downarrow})$] in the transversal terminals 2 and 4. Here the boundary conditions for the four terminals are $\mu_{1\uparrow} = \mu_{1\downarrow} = eV/2$, $\mu_{2\uparrow} = \mu_{2\downarrow} = 0$, $\mu_{3\uparrow} = \mu_{3\downarrow} = -eV/2$, and $\mu_{4\uparrow} = \mu_{4\downarrow} = 0$. The currents in the terminals 2 and 4 satisfy the relations: $I_{2e} = -I_{4e} \equiv I_e$ and $I_{2s} = -I_{4s} \equiv I_s$. Figures 1(a) and 1(b) show the Hall conductance I_e/V and spin Hall conductance I_s/V versus the Dirac-point energy ϵ_0, respectively. For a nonferromagnetic graphene ($M = 0$) under the high magnetic field ($\phi = 0.005$), I_s/V is zero and I_e/V exhibits the plateaus at odd integer values ne^2/h ($n = \pm1, \pm3, \ldots$) due to the quantum Hall effect (QHE). These results have been observed in recent experiments [14,15]. For a ferromagnetic graphene with $M \neq 0$, the spin current emerges [see Fig. 1(b)] since the QSHE. The spin Hall conductance I_s/V also shows the quantized plateaus. By considering the edge state under the high magnetic field, the plateau values of I_s/V and I_e/V can be analytically derived to be at ($\nu_\uparrow - \nu_\downarrow)e/8\pi$ and ($\nu_\uparrow + \nu_\downarrow)e^2/2h$ [22], where ν_σ is the Landau filling factor for spin σ. In particular, when $|\epsilon_0| < |M|$, in which case the Fermi energy E_F ($E_F = 0$) is located between the spin-up Dirac point $\epsilon_0 - M$ and the spin-down Dirac point $\epsilon_0 + M$, I_e is zero and a net quantum spin current emerges in the transversal terminals. In addition, if in the open circuit case, the spin accumulation emerges at the sample boundaries instead of the spin current [22].

Since the QSHE can give rise to quantum plateaus in resistances, we next study the longitudinal and Hall resistances in the six-terminal Hall device [see the inset in the lower left corner of Fig. 1(a)]. Now we consider a small bias V applied to the longitudinal terminals 1 and 4. The transversal terminals 2, 3, 5, and 6 are all voltage probes, their charge currents vanish ($I_{pe} = 0$) and $\mu_{p\uparrow} = \mu_{p\downarrow} \equiv \mu_p$. Combining these boundary conditions with the Landauer-Büttiker formula, the voltages V_p ($V_p = \mu_p/e$) in four voltage probes can be obtained, then the longitudinal resistance $R_{14,23} = (V_2 - V_3)/I_{14}$ and Hall resistance $R_{14,26} = (V_2 - V_6)/I_{14}$ are calculated, here $I_{14} = -I_{1e} = I_{4e}$. The resistances contain the properties $R_{14,26} = R_{14,35}$ and $R_{14,23} = R_{14,65}$.

Figures 2(a) and 2(b) show the longitudinal and Hall resistances, $R_{14,23}$ and $R_{14,26}$, versus the energy ϵ_0 and the exchange split M at an external magnetic field $\phi = 0.005$. Because of the QSHE and QHE, both $R_{14,23}$ and $R_{14,26}$ may

FIG. 2 (color). The panels (a) and (b) show the resistances $R_{14,23}$ and $R_{14,26}$ (in the unit of h/e^2) vs the exchange split M and energy ϵ_0 for $N = 80$ and $\phi = 0.005$.

FIG. 3 (color online). The resistances $R_{14,23}$ (a) and $R_{14,26}$ (b) vs the energy ϵ_0 for $N = 80$ and $\phi = 0.005$.

be nonzero, and they both exhibit plateau structures. The plateau values are determined by the filling factors $\nu_\uparrow$ and $\nu_\downarrow$. For the fixed filling factors $\nu_\uparrow$ and $\nu_\downarrow$, $R_{14,23}$ and $R_{14,26}$ maintain their plateau values regardless of ϵ_0 and M. By considering the carriers transport along the edge states, the plateau values can be analytically derived [22] $R_{14,23} = 0$ and $R_{14,26} = [1/(\nu_\uparrow + \nu_\downarrow)]h/e^2$ for $(\nu_\uparrow, \nu_\downarrow) = (+, +)$ or $(-, -)$, and $R_{14,23} = [|\nu_\uparrow \nu_\downarrow|/(|\nu_\uparrow|^3 + |\nu_\downarrow|^3)]h/e^2$ and $R_{14,26} = \text{sign}(\nu_\uparrow)[(|\nu_\uparrow|^2 - |\nu_\downarrow|^2)/(|\nu_\uparrow|^3 + |\nu_\downarrow|^3)]h/e^2$ for $(\nu_\uparrow, \nu_\downarrow) = (+, -)$ or $(-, +)$. Some plateau values for low $\nu_\uparrow$, $\nu_\downarrow$ have been labeled in Fig. 2. The numerical results in Fig. 2 are in excellent agreement with the analytic plateau values (the differences between them are less than 10^{-6}). Furthermore, $R_{14,23}$ and $R_{14,26}$ have the following properties: While $|\epsilon_0| > |M|$ with $(\nu_\uparrow, \nu_\downarrow) = (+, +)$ or $(-, -)$, the longitudinal resistance $R_{14,23}$ is zero and only the Hall resistance $R_{14,26}$ exists because the spin-up and spin-down carriers are simultaneously either electronlike or holelike and move in the same direction. On the other hand, while $|\epsilon_0| < |M|$ with $(\nu_\uparrow, \nu_\downarrow) = (+, -)$ or $(-, +)$, the Fermi energy E_F is located between $\epsilon_0 + M$ and $\epsilon_0 - M$, the longitudinal resistance $R_{14,23}$ emerges since now the spin-up and spin-down carriers move in opposite directions for a given edge. (i) While $\nu_\uparrow = -\nu_\downarrow \equiv \nu$, the Hall resistance $R_{14,26} = 0$, only the longitudinal resistance $R_{14,23}$ exists with the value $(1/2\nu)h/e^2$. This means that only the QSHE emerges and the QHE vanishes in this region. In this case, the system has the CT invariance. Furthermore, if $\nu_\uparrow = -\nu_\downarrow = \pm 1$, $R_{14,26} = 0$, and $R_{14,23} = (1/2)(h/e^2)$. Now the observed phenomena are completely the same with the QSHE from the SOI [5–7,9,10], but their physical

mechanisms are different. (ii) While $\nu_\uparrow \neq -\nu_\downarrow$ but still with $(\nu_\uparrow, \nu_\downarrow) = (+, -)$ or $(-, +)$, $R_{14,26}$ is now nonzero since the numbers of the spin-up and spin-down edge states are different. In this case, both resistances $R_{14,26}$ and $R_{14,23}$ have nonzero quantized plateaus and the QSHE and QHE coexist. Figure 3 shows the resistances $R_{14,23}$ and $R_{14,26}$ versus the energy ϵ_0 for a fixed M (i.e., along the horizontal lines in Fig. 2), and it clearly shows that the quantum plateaus persist very well.

Up to now, we demonstrate the existence of QSHE in the ferromagnetic graphene from both physical picture and detailed numerical calculations. In the following, we study the properties of the spin Hall resistance R_s, a measurable quantity robust to dephasing [23]. and well reflecting the topological invariance of the system. We again consider the four-terminal Hall bar. But now the transversal terminals 2 and 4 are spin-biased probes with boundary conditions $I_{p\uparrow} = I_{p\downarrow} = 0$ ($p = 2, 4$). Here the spin Hall resistance R_s is defined as the transversal spin bias over the longitudinal charge current: $R_s \equiv (\mu_{2\uparrow} - \mu_{2\downarrow})/eI_{13} = -(\mu_{4\uparrow} - \mu_{4\downarrow})/eI_{13}$. Since the spin bias $\mu_{n\uparrow} - \mu_{n\downarrow}$ is experimentally measurable, so is the R_s [24,25]. Figure 4 shows R_s versus the energy ϵ_0 for different ferromagnetic exchange split M and magnetic field ϕ. For $|\epsilon_0| > |M|$ with $(\nu_\uparrow, \nu_\downarrow) = (+, +)$ or $(-, -)$, $R_s = 0$. On the other hand, while $|\epsilon_0| < |M|$ with $(\nu_\uparrow, \nu_\downarrow) = (+, -)$ or $(-, +)$, R_s exists. R_s exhibits the quantum plateaus, and its plateau values are at $[1/(|\nu_\uparrow| + |\nu_\downarrow|)]h/e^2$. For a small M (e.g., $M = 0.02t$ or $0.05t$ in Fig. 4(b)) or a high magnetic field ϕ [e.g., $\phi = 0.005$ in Fig. 4(a)], $(\nu_\uparrow, \nu_\downarrow)$ can only equal to

FIG. 4 (color online). (a) shows R_s vs ϵ_0 for $M = 0.05$ and (b) shows R_s vs ϵ_0 for $\phi = 0.005$. The parameter $N = 80$.

FIG. 5 (color online). R_s vs ϵ_0 (a) and R_s vs the disorder strength W (b) with the parameters $N = 40$, $\phi = 0.007$, and $M = 0.05$. The curves in (a) and (b) are averaged over up to 1000 and 8000 random configurations, respectively.

$(1, -1)$, so only the plateau of $R_s = h/2e^2$ emerges. But for a large M or a small magnetic field ϕ, $(\nu_\uparrow, \nu_\downarrow)$ may be $(1, -3)$, $(3, -1)$, $(1, -5)$, $(5, -1)$, etc., then the plateaus of $R_s = h/4e^2$, $h/6e^2$, etc., are also possible.

Finally, we examine the disorder effect on the spin Hall resistance R_s. Here we assume that the disorder only exists in the central region [see dotted box in top right inset of Fig. 1(a)]. Because of the disorder, the on-site energy $\epsilon_0 - \sigma M$ for each site i in the central region is changed to $\epsilon_0 + w_i - \sigma M$, where w_i is uniformly distributed in the range $[-W/2, W/2]$ with the disorder strength W. Figure 5(a) shows R_s versus the energy ϵ_0 at the different disorder strengths W and Fig. 5(b) shows R_s versus the disorder strength W at different energies ϵ_0. The results show that the quantum plateaus of R_s are very robust against the disorder because of the topological invariance of the system. The quantum plateau maintains its quantized value very well even when W reaches 2 [see Figs. 5(a) and 5(b)]. Since the plateau is so robust and stable, its value can be used as the standard for the spin Hall resistance. In addition, even for a very large disorder strength W (e.g., $W = 5$ or larger), the plateau value only slightly decreases while maintaining the plateau structure [see Fig. 5(b)]. This is because although the disorder strongly weakens the spin bias $\mu_{2\uparrow} - \mu_{2\downarrow}$, it also weakens the longitudinal charge current I_{13}, so the value of R_s is affected less. This means that in the large disorder limits ($W \rightarrow \infty$), although the QSHE is broken, the SHE still holds.

In summary, we predict a new QSHE in the ferromagnetic graphene film. Unlike the QSHEs studied so far, the origin of this QSHE is not caused by the spin-orbit interaction. The results also show that the system can exhibit the QSHE, the QHE, and the coexistence of the QSHE and QHE, depending on the filling factors of the spin-up and spin-down carriers. Because of the QSHE and QHE, both the longitudinal and Hall resistances exhibit the plateau structures. The plateau values (in the unit of h/e^2) are at $1/2$, $1/6$, $3/28$, ..., for the longitudinal resistance and at $\pm 1/2$, $\pm 1/4$, $\pm 1/6$, $\pm 2/7$, ..., for the Hall resistance. In addition, the spin Hall resistance has also investigated and found to be robust against the disorder.

*sunqf@aphy.iphy.ac.cn

[1] M. I. Dyakonov and V. I. Perel, JETP Lett. **13**, 467 (1971).
[2] J. E. Hirsch, Phys. Rev. Lett. **83**, 1834 (1999).
[3] S. Murakami, N. Nagaosa, and, S. C. Zhang, Science **301**, 1348 (2003); J. Sinova et al., Phys. Rev. Lett. **92**, 126603 (2004).
[4] Y. K. Kato et al., Science **306**, 1910 (2004); J. Wunderlich et al., Phys. Rev. Lett. **94**, 047204 (2005).
[5] C. L. Kane and E. J. Mele, Phys. Rev. Lett. **95**, 146802 (2005).
[6] C. L. Kane and E. J. Mele, Phys. Rev. Lett. **95**, 226801 (2005).
[7] C. Day, Phys. Today **61**, No. 1, 19 (2008); N. Nagaosa, Science **318**, 758 (2007).
[8] H. Min et al., Phys. Rev. B **74**, 165310 (2006); Y. Yao et al., Phys. Rev. B **75**, 041401(R) (2007).
[9] L. Sheng et al., Phys. Rev. Lett. **95**, 136602 (2005); B. A. Bernevig and S.-C. Zhang, Phys. Rev. Lett. **96**, 106802 (2006); L. Fu, C. L. Kane, and E. J. Mele, Phys. Rev. Lett. **98**, 106803 (2007); C. Liu et al., Phys. Rev. Lett. **100**, 236601 (2008).
[10] B. A. Bernevig, T. L. Hughes, and S. C. Zhang, Science **314**, 1757 (2006).
[11] M. König et al., Science **318**, 766 (2007).
[12] D. Hsieh et al., Nature (London) **452**, 970 (2008).
[13] C. W. J. Beenakker, Rev. Mod. Phys. **80**, 1337 (2008); A. H. Castro Neto et al., Rev. Mod. Phys. **81**, 109 (2009).
[14] K. S. Novoselov et al., Science **306**, 666 (2004); Nature (London) **438**, 197 (2005); Nature Phys. **2**, 177 (2006).
[15] Y. Zhang et al., Nature (London) **438**, 201 (2005).
[16] Y.-W. Son et al., Nature (London) **444**, 347 (2006); E.-J. Kan et al., Appl. Phys. Lett. **91**, 243116 (2007).
[17] H. Haugen, D. Huertas-Hernando, and A. Brataas, Phys. Rev. B **77**, 115406 (2008); J. Linder et al., Phys. Rev. Lett. **100**, 187004 (2008).
[18] Q. Zhang et al., Phys. Rev. Lett. **101**, 047005 (2008).
[19] W. Long, Q. F. Sun, and J. Wang, Phys. Rev. Lett. **101**, 166806 (2008).
[20] *Electronic Transport in Mesoscopic Systems*, edited by S. Datta (Cambridge University Press, Cambridge, England, 1995).
[21] D. H. Lee and J. D. Joannopoulos, Phys. Rev. B **23**, 4997 (1981); M. P. Lopez Sancho et al., J. Phys. F **14**, 1205 (1984); **15**, 851 (1985).
[22] See supplementary material at http://link.aps.org/supplemental/10.1103/PhysRevLett.104.066805.
[23] H. Jiang et al., Phys. Rev. Lett. **103**, 036803 (2009).
[24] E. J. Koop et al., Phys. Rev. Lett. **101**, 056602 (2008); Q.-F. Sun, Y. Xing, and S. Q. Shen, Phys. Rev. B **77**, 195313 (2008); Y. X. Xing, Q.-F. Sun, and J. Wang, Appl. Phys. Lett. **93**, 142107 (2008).
[25] S. M. Frolov et al., Phys. Rev. Lett. **102**, 116802 (2009); Nature (London) **458**, 868 (2009).